



HAL
open science

Historical carbon dioxide emissions caused by land-use changes are possibly larger than assumed

Almut Arneth, Stephen Sitch, Julia Pongratz, B. D. Stocker, Philippe Ciais, B. Poulter, A. D. Bayer, Alberte Bondeau, L. Calle, L. P. Chini, et al.

► To cite this version:

Almut Arneth, Stephen Sitch, Julia Pongratz, B. D. Stocker, Philippe Ciais, et al.. Historical carbon dioxide emissions caused by land-use changes are possibly larger than assumed. *Nature Geoscience*, 2017, 10 (2), pp.79-84. 10.1038/NGEO2882. hal-01681571

HAL Id: hal-01681571

<https://hal.science/hal-01681571v1>

Submitted on 14 May 2018

HAL is a multi-disciplinary open access archive for the deposit and dissemination of scientific research documents, whether they are published or not. The documents may come from teaching and research institutions in France or abroad, or from public or private research centers.

L'archive ouverte pluridisciplinaire **HAL**, est destinée au dépôt et à la diffusion de documents scientifiques de niveau recherche, publiés ou non, émanant des établissements d'enseignement et de recherche français ou étrangers, des laboratoires publics ou privés.

9-2

1 **Historical carbon dioxide emissions due to land use changes possibly larger than assumed**

2 A Arneth (1), S Sitch (2), J Pongratz (3), B Stocker (4,5), P Ciais (6), B Poulter (7), A Bayer
3 (1), A Bondeau (8), L Calle (7), L. Chini (9), T Gasser (6), M Fader (8,10), P Friedlingstein (11), E
4 Kato (12), W Li (6), M Lindeskog (13), J E M S Nabel (3), TAM Pugh (1, 14), E Robertson (15), N
5 Viovy (6), C Yue (6), S Zaehle (16)

6

7 (1) Karlsruhe Institute of Technology, Dept. Atmospheric Environmental Research, Kreuzteckbahnstr.
8 19, 82467 Garmisch-Partenkirchen, Germany

9 (2) College of Life and Environmental Sciences, University of Exeter, Exeter, EX4 4RJ, UK

10 (3) Max Planck Institute for Meteorology, Bundesstr. 53, 20146 Hamburg, Germany

11 (4) Department of Life Sciences and Grantham Institute for Climate Change, Imperial College
12 London, Silwood Park, Ascot, SL5 7PY, UK

13 (5) Institute for Atmospheric and Climate Science, ETH Zürich, Universitätstrasse 16, 8092 Zürich,
14 Switzerland

15 (6) IPSL – LSCE, CEA CNRS UVSQ, Centre d'Etudes Orme des Merisiers, 91191 Gif sur Yvette
16 France

17 (7) Institute on Ecosystems and Department of Ecology, Montana State University, Bozeman, MT
18 59717

19 (8) Institut Méditerranéen de Biodiversité et d'Ecologie marine et continentale, Aix-Marseille
20 Université, CNRS, IRD, Avignon Université, Technopôle Arbois-Méditerranée, Bâtiment Villemin,
21 BP 80, 13545 Aix-en-Provence CEDEX 04, France

22 (9) Department of Geographical Sciences, University of Maryland, College Park, MD 20742, USA

23 (10) International Centre for Water Resources and Global Change, hosted by the German Federal
24 Institute of Hydrology. Am Mainzer Tor 1, 56068 Koblenz, Germany

25 (11) College of Engineering, Mathematics and Physical Sciences, University of Exeter, Exeter, EX4
26 4QE, UK

27 (12) The Institute of Applied Energy, Minato, Tokyo 105-0003, Japan

28 (13) Dept of Physical Geography and Ecosystem Science, Sölvegatan 12, Lund University,
29 22362 Lund, Sweden

30 (14) School of Geography, Earth & Environmental Sciences and Birmingham Institute of Forest
31 Research, University of Birmingham, Birmingham, B15 2TT, United Kingdom

32 (15) Met Office Hadley Centre, FitzRoy Road, Exeter, EX1 3PB, UK

33 (16) Max Planck Institute for Biogeochemistry, 07701 Jena, Germany

34

35

36

37 **The terrestrial biosphere absorbs about 20% of fossil fuel CO₂ emissions. The overall**
38 **magnitude of this sink is constrained by the difference between emissions, the rate of**
39 **increase in atmospheric CO₂ concentrations and the ocean sink. However, the land sink**
40 **is actually composed of two largely counteracting fluxes that are poorly quantified:**
41 **fluxes from land-use change and CO₂ uptake by terrestrial ecosystems. Dynamic global**
42 **vegetation model simulations suggest that CO₂ emissions from land-use change have**
43 **been substantially underestimated because processes such as tree harvesting and land-**
44 **clearing from shifting cultivation have not been considered. Since the overall terrestrial**
45 **sink is constrained, a larger net flux as a result of land-use change implies that**
46 **terrestrial uptake of CO₂ is also larger, and that terrestrial ecosystems might have**
47 **greater potential to sequester carbon in the future. Consequently, reforestation projects**
48 **and efforts to avoid further deforestation could represent important mitigation**
49 **pathways, with co-benefits for biodiversity. It is unclear whether a larger land carbon**
50 **sink can be reconciled with our current understanding of terrestrial carbon cycling. In**
51 **light of our possible underestimation of the historical residual terrestrial carbon sink**
52 **and associated uncertainties, we argue that projections of future terrestrial carbon**
53 **uptake and losses are more uncertain than ever.**

54

55 The net atmosphere-to-land carbon flux (F_L) is typically inferred as the difference between relatively
56 well-constrained terms of the global carbon cycle: fossil fuel and cement emissions, oceanic carbon
57 uptake and atmospheric growth rate of CO₂ (see Textbox) ¹. In contrast, very large uncertainties exist
58 in how much anthropogenic land-use and land-cover change (F_{LULCC}) contributes to F_L , which
59 propagates into large uncertainties in the estimation of the residual carbon flux (F_{RL}) (Box 1). The lack
60 of confidence in separating F_L into its component fluxes diminishes the predictive capacity for
61 terrestrial carbon cycle projections into the future. It restricts our ability to estimate the capacity of

62 land ecosystems to continue to mitigate climate change, and to assess land management options for
63 land-based mitigation policies.

64 As land-use change emissions and the residual sink are spatially closely enmeshed, global-scale
65 observational constraints do not exist for estimating F_{LULCC} or F_{RL} separately. Dynamic Global
66 Vegetation Models (DGVMs) have over recent years been used to infer the magnitude and spatial
67 distribution of F_{LULCC} as well as of F_{RL} , while F_{LULCC} has traditionally been also derived from data-
68 driven approaches such as the bookkeeping method¹⁻³ (Box 1). Although large, for some sources of
69 uncertainties in F_{LULCC} (such as differences in baseline years used for calculation, how environmental
70 effects have been considered, or assumptions about wood products) there is no good reason to believe
71 that these would introduce a systematic under- or overestimation⁴⁻⁶. However, until recently, most
72 processes related to land management and the subgrid-scale dynamics of land-use change have been
73 ignored in large-scale assessments of the terrestrial carbon balance, and we argue here that including
74 these missing processes might systematically increase the magnitude of F_{LULCC} . In turn, an upward
75 revision of F_{LULCC} implies through the global budget the existence of a substantially higher F_{RL} and
76 raises the question whether this is plausible given our understanding of the response of ecosystems to
77 changing environmental conditions.

78 **Gross land-cover transitions such as shifting cultivation**

79 Opposing changes in different land-use types can take place simultaneously within a region (see
80 Methods and Supplementary Figure 1), for example: an area might be converted from natural to
81 managed land, whereas an equal area within the same region might be abandoned or reforested,
82 equating to a net-zero land-cover change. The magnitude of these bi-directional changes depends on
83 the size of the area investigated. Over thousands of kilometres squared (the typical resolution of
84 DGVMs), ignoring sub-grid changes can have a substantial effect on the simulated carbon cycle, since
85 accounting for the gross changes (for example, the parallel conversion to, and abandonment of,
86 agricultural land in the same grid-cell) includes (rapid) carbon losses from deforestation, (slow) loss
87 from post-deforestation soil-legacy effects, and (slow) uptake in areas of regrowth. In sum this leads to

88 younger mean stand age, smaller biomass pools and thus higher F_{LULCC} compared to net area-change
89 simulations.

90 Gross area transitions are fundamental to land-use land-cover change (LULCC) dynamics in areas of
91 shifting cultivation (SC) in the tropics⁷, but also occur elsewhere⁸. Gross forest loss far exceeding net
92 area loss can be demonstrated from remote-sensing products globally⁹, although these products in
93 themselves cannot distinguish effects of logging from natural disturbance events such as fire or
94 storms. Secondary forests in the tropics can return to biomass carbon stocks comparable to old-growth
95 forest within five to six decades¹⁰, but the same is not the case for soil carbon. Also, fallow lengths in
96 SC systems tends to be shorter, and show a decreasing trend in many regions¹¹. These dynamics result
97 in the degraded vegetation and reduced soil carbon stocks commonly observed in disturbed forest land
98 ¹².

99 **Wood harvesting**

100 Until recently, global DGVM studies that accounted for LULCC concentrated on the representation of
101 conversion of natural lands to croplands and pastures, while areas under forest cover were represented
102 as natural forest, and hence by each model's dynamics of establishment, growth and mortality. Two-
103 thirds to three-quarters of global forests have been affected by human use, which is mainly due to
104 timber harvest; but forests are also a source of firewood or secondary products; or used for recreational
105 purposes¹³. Between 1700-2000 an estimated 86 PgC has been removed globally from forests due to
106 wood harvesting (WH)¹⁴. WH leads to reduced carbon density on average in managed forests¹⁵ and
107 can ultimately result in degradation in the absence of sustainable management strategies. Furthermore,
108 the harvest of wood can reduce litter input, which lowers soil pools¹³. Bringing a natural forest under
109 any harvesting regime probably will lead to net-CO₂ emissions to the atmosphere – with a magnitude
110 and time-dependency conditionnal on harvest intensity and frequency, regrowth and the fate and
111 residence time of the wood products.

112 **Grazing and crop harvesting, and cropland management**

113 Management is not only fundamental for the carbon balance of forests, but also for pasture and
114 cropland. As with forests, accounting for management processes on arable lands has only recently
115 been included in DGVMs (see Methods). Regular grazing and harvesting (GH), and more realistic
116 crop management processes (MC) such as flexible sowing and harvesting, or tillage, will enhance
117 F_{LULCC} (ref. 16). Over decadal timescales, conversion of forest to cropland has been observed to reduce
118 soil carbon pools by around 40% (ref. 17), resulting from reduced vegetation litter soil inputs and
119 enhanced soil respiration in response to tillage, although the effect and magnitude of the latter is being
120 debated¹⁸. Conversion to pasture often has either little effect, or may even increase soil carbon¹⁷.

121 **Impacts of land-management processes on the carbon cycle**

122 The few published DGVM studies that account for the management of land more realistically^{16,19-21}
123 consistently suggest a systematically larger F_{LULCC} over the historical period compared to estimates
124 that ignored these processes, with important implications for our understanding of the terrestrial
125 carbon cycle and its role for historical (and future) climate change. In order to assess if results from
126 these initial experiments hold despite differences among models, we compile here results from a wider
127 set of DGVMs (and one DGVM “emulator”, see Methods and Supplementary Table 1), adopting the
128 approach described in ref. 2. F_{LULCC} was calculated as the difference between a simulation in which
129 CO₂ and climate were varied over the historical period, at constant (pre-industrial) land use, and one in
130 which land use was varied as well.

131 When accounting for SC and WH, F_{LULCC} was systematically enhanced (Fig. 1). Shifting-
132 cultivation, assuming that no shade-trees remain in cultivated areas, results in increased cumulative
133 F_{LULCC} over the period 1901-2014 on average by 35 ± 18 PgC (Fig. 1, Supplementary Table 2).
134 Although three DGVMs had demonstrated this effect previously¹⁹⁻²¹, an upward shift of F_{LULCC} was
135 also found in the other models that performed additional SC simulations for this study. Including WH
136 caused F_{LULCC} to increase over the same time period by a similar magnitude to SC: 30 ± 21 PgC.

137 Trends in WH-related F_{LULCC} over time differed between models (Fig. 1) probably due to different
138 rates of post-harvest regrowth, and assumptions about residence time in different pools²². Including the
139 harvesting of crops and the grazing of pastures also resulted in larger F_{LULCC} , as carbon harvested or
140 grazed is consumed and released as CO₂ rapidly instead of decaying slowly as litter and soil organic
141 matter. Beyond harvest, accounting for more realistic MC such as tillage processes also showed, with
142 one exception (in which tillage effects were not modelled, see methods) an enhancement of F_{LULCC}
143 emissions.

144 When ignoring the additional land-use processes investigated here, average F_{LULCC} is 119 ± 50 PgC
145 (Supplementary Table 2). Adding effects of SC, WH, GH and MC enhance land-use change emissions
146 by, on average, 20-30% each (Fig. 2; Supplementary Table 1), with individually large uncertainties.
147 The combined effects on F_{LULCC} are difficult to judge as models do not yet account for all land-use
148 dynamics. For instance, SC and WH effects are expected to enhance F_{LULCC} additively as there is little
149 overlap in the input dataset used by DGVMs regarding the areas that are assumed to be under SC, and
150 areas where other types of forest harvesting occur⁷. But in the case of accounting for harvesting and
151 other management on arable lands and pastures, carbon cycle interactions with SC and WH cannot be
152 excluded because subsequent transitions could occur in a grid location, between primary vegetation
153 and cropland, pastures or secondary forests. The overall enhancement of F_{LULCC} therefore, will need to
154 be explored with model frameworks that include all dynamic land-use-change processes. DGVMs
155 currently contributing to the annual update of the global carbon budget account for some of the
156 processes examined here, but as of yet not at all comprehensively, and we thus expect DGVM-based
157 F_{LULCC} to increase substantially compared to results reported in ref. 1. As a consequence, the
158 discrepancy to bookkeeping estimates of F_{LULCC} will become larger, although results in ref. 23 call for
159 a broader range of bookkeeping approaches as well.

160 **Implications for the historical residual land sink**

161 In order to match F_L in the global carbon budget (Box 1) for the historical period a substantially larger
162 F_{LULCC} would need to be balanced by a corresponding increase in F_{RL} , which could be either due to

163 underestimated historical increase in gross primary production (GPP) and vegetation biomass,
164 overestimated heterotrophic carbon loss, or both. The question arises if such a discrepancy is credible
165 in light of today's understanding. For instance, by compiling a number of observations Pan et al.²⁴
166 suggested a forest sink that is in line with total carbon budget estimates¹. However, their study
167 excluded savannahs, grasslands, and woodlands and in semi-arid regions alone carbon uptake was
168 estimated to be about 20% of the terrestrial sink (plus around another 30% from other non-forested
169 ecosystems), which also dominate the recent positive trend in carbon uptake²⁵. Reconstructing the
170 Austrian historical forest sink from inventory data also suggested a much larger residual sink,
171 compared with (bookkeeping) model results²⁶.

172 The response of photosynthesis to increasing CO₂ could underlie more than half of today's land carbon
173 sink²⁷. Several recent lines of observation-based evidence suggest that GPP may have undergone much
174 stronger enhancement over the last century than currently calculated by DGVMs. These studies
175 include isotopic analysis of herbarium plant samples, of stable oxygen isotope ratios in atmospheric
176 CO₂, and accounting for the effect of leaf mesophyll resistance to CO₂ (refs 28-30). Ciais *et al.*³¹
177 inferred a pre-industrial GPP of 80 PgC a⁻¹ based on measurements of oxygen isotopes in ice-core air,
178 indicative for a 33% difference to the often-used present-day GPP benchmark of ~120 PgC a⁻¹ (ref. 32)
179 and independently consistent with the 35% increase suggested by ref. 28. In contrast, the participating
180 DGVMs in this study show an average increase of GPP by only 15% between the first and last ten
181 years of the simulation (not shown).

182 Whether or not enhancements in GPP translate into increased carbon storage depends on other factors
183 such as nutrient and water supply, seen for instance in the mixed trends in stem growth found in forest
184 inventories^{33,34}. Much work remains to better understand the response of ecosystem carbon storage to
185 increasing atmospheric CO₂ concentration³⁵. Ultimately, carbon turnover time determines whether or
186 not enhanced growth will only result in increasing carbon pools²². Besides GPP and heterotrophic
187 ecosystem respiration, lateral carbon flows play an important role in the ecosystem carbon sink.
188 Recent syntheses that combined a range of observations, inventories of carbon stock changes, trade

189 flows and transport in waterways, estimated dissolved organic carbon losses to account for a flux of >
190 1.0 PgC a⁻¹, with an unknown historical trend^{36,37}. The fate of this carbon is highly uncertain, but its
191 inclusion would enhance the calculated residual sink via an additional loss term (Box 1, equation (1)).
192 Taken together, a number of candidates for underestimated F_{RL} in today's models are plausible, and a
193 combination of the above listed processes likely. It remains to be seen whether a larger F_{LULCC} can be
194 supported by observation-based estimates. Several lines of evidence suggest that a common low-bias
195 in the historic F_{LULCC} could affect all DGVMs, and the challenge of resolving the many open issues
196 will stay with us for some years to come.

197 **Unknowns in historical LULCC reconstructions**

198 Patterns and historical trends of deforestation, cropland and pasture management, or WH are
199 uncertain. Land-use reconstructions differ substantially in terms of the time, location and rate of
200 LULCC (see ref. 38 and reference therein). The DGVM and climate science community has mostly
201 relied on the LUH1 dataset by Hurtt et al.⁷, chiefly because it provides the needed seamless time series
202 from the historical period into future projections at the spatial resolution required by DGVMs. Clearly
203 such a globally applicable gridded dataset must necessarily include simplifications. For instance, the
204 assumed uniform 15-year turnover in tropical SC systems⁷ cannot account for the known variation
205 between a few years and one to two decades, or trends towards shorter fallow periods in some regions
206 (see ref. 11 and references therein), although there is also an increasing proportion of permanent
207 agriculture. Likewise, not only the amount of WH but also the type of forestry (coppice, clear-cut,
208 selective logging, fuel-wood) will vary greatly in time and space, which is difficult to hindcast^{39,40}.

209 In upcoming revisions to LUH1 (LUH-2, <http://luh.umd.edu/data.shtml>), forest-cover gross
210 transitions are now constrained by the remote sensing information⁹, and have overall been re-estimated
211 (Fig. 3). Whether or not this will result in reduced SC carbon loss estimates in recent decades remains
212 to be seen. At the same time, these historical estimates consider large gross transitions of land-cover
213 change only for tropical regions even though there is good reason to believe that bi-directional
214 changes occur elsewhere⁴¹. For Europe alone, a recent assessment that is relatively impartial to spatial

215 resolution estimated twice the area having undergone land-use transitions since 1900 when accounting
216 for gross *vs.* net area changes⁸. This leads to substantial increase in the calculated historical European
217 F_{LULCC} , both in a bookkeeping-model and DGVM-based study⁴². Historical land carbon cycle
218 estimates therefore are not only highly uncertain due to missing LULCC processes, but equally so due
219 to the LULCC reconstructions *per se*. However, for a given reconstruction, accounting for additional
220 processes discussed here will always introduce a unidirectional enhancement in F_{LULCC} compared to
221 ignoring these processes.

222 **Implications for the future land carbon mitigation potential**

223 Our calculated increases in F_{LULCC} , in absence of a clear understanding of the processes underlying
224 F_{RL} , notably strengthen the existing arguments to avoid further deforestation (and all ecosystem
225 degradation) – an important aspect of climate change mitigation, with considerable co-benefits to
226 biodiversity and a broad range of ecosystem service supply. One could also conjecture whether or not
227 a larger historical carbon loss through LULCC would imply a larger potential to sequester carbon
228 through reforestation, than thought so far. However, assessments of mitigation potentials must
229 consider the often relatively slow carbon gain in regrowing forests (compared to the rapid, large loss
230 during deforestation), in particular the sluggish replenishment of long-term soil carbon storage^{43,44}.
231 What is more, trees grow now, and will in future, under very different environmental conditions
232 compared to the past. A warmer climate increases mineralisation rates and hence enhances nutrient
233 supply to plant growth, supporting the CO₂ fertilisation effect, but also stimulates heterotrophic decay
234 of existing soil carbon and/or flow of dissolved carbon, with as yet no agreement about the net
235 effects^{3,45}. Regrowing forests might also in future be more prone to fire risk, and other episodic events
236 such as wind-throw or insect outbreaks^{46,47}, crucial ecosystem features not yet represented well in
237 models⁴⁸. This question of “permanence” has been an important point of discussion at conferences
238 under the UNFCCC, and also endangers the success of payment-for-ecosystem-services schemes that
239 target conservation measures, as it is unclear how an increasing risk of losing carbon-uptake potential
240 can be accounted for^{49,50}.

241 Given that we may be greatly underestimating the present-day F_{RL} , and therefore missing or
242 underestimating the importance of key driving mechanisms, projections of future terrestrial carbon
243 uptake and losses appear more fraught with uncertainty than ever. In the light of the findings
244 summarized here, this poses not only a major challenge when judging mitigation efforts, but also for
245 the next generation of DGVMs and Earth System models to assess the future global carbon budget.
246 Future work therefore needs to concentrate on representing the interactions between physiological
247 responses to environmental change in ecosystems with improved representations of human land
248 management.

249

250 **References**

251

- 252 1 Le Quere, C. *et al.* Global Carbon Budget 2015. *Earth Sys. Sci. Data* 7, 349-396 (2015).
- 253 2 Sitch, S. *et al.* Recent trends and drivers of regional sources and sinks of carbon dioxide.
254 *Biogeosciences* 12, 653-679 (2015).
- 255 3 Ciais, P. *et al.* in *Climate Change 2013: The Physical Science Basis. Contribution of Working*
256 *Group I to the Fifth Assessment Report of the Intergovernmental Panel on Climate Change.*
257 (eds T.F. Stocker *et al.*) (Cambridge University Press, 2013).
- 258 4 Pongratz, J., Reick, C., Houghton, R. A. & House, J. I. Terminology as a key uncertainty in
259 net land use flux estimates. *Earth Syst. Dyn.* 5, 177-195 (2013).
- 260 5 Gasser, T. & Ciais, P. A theoretical framework for the net land-to-atmosphere CO₂ flux and its
261 implications in the definitions of "emissions from land-use change". *Earth Syst. Dyn.* 4, 171-
262 186 (2013).
- 263 6 Houghton, R. A. *et al.* Carbon emissions from land use and land-cover change.
264 *Biogeosciences* 9, 5125-5142 (2012).

- 265 7 Hurtt, G. C. *et al.* Harmonization of land-use scenarios for the period 1500-2100: 600 years of
266 global gridded annual land-use transitions, wood harvest, and resulting secondary lands. *Clim.*
267 *Change* 109, 117-161 (2011).
- 268 8 Fuchs, R., Herold, M., Verburg, P. H., Clevers, J. G. P. W. & Eberle, J. Gross changes in
269 reconstructions of historic land cover/use for Europe between 1900 and 2010. *Glob. Change*
270 *Biol.* 21, 299-313 (2015).
- 271 9 Hansen, M. C., Stehman, S. V. & Potapov, P. V. Quantification of global gross forest cover
272 loss. *Proc. Nat. Acad. Sci.* 107, 8650-8655 (2010).
- 273 10 Poorter, L. *et al.* Biomass resilience of Neotropical secondary forests. *Nature* 530, 211-214
274 (2016).
- 275 11 van Vliet, N. *et al.* Trends, drivers and impacts of changes in swidden cultivation in tropical
276 forest-agriculture frontiers: A global assessment. *Glob. Env. Change* 22, 418-429 (2012).
- 277 12 Grace, J., Mitchard, E. & Gloor, E. Perturbations in the carbon budget of the tropics. *Glob.*
278 *Change Biol.* 20, 3238-3255 (2014).
- 279 13 Erb, K.-H. *et al.* Land management: data availability and process understanding for global
280 change studies. *Glob. Change Biol.*, gcb.13443 (2016).
- 281 14 Hurtt, G. C. *et al.* The underpinnings of land-use history: three centuries of global gridded
282 land-use transitions, wood-harvest activity, and resulting secondary lands. *Glob. Change Biol.*,
283 12, 1208-1229 (2006).
- 284 15 Noormets, A. *et al.* Effects of forest management on productivity and carbon sequestration: A
285 review and hypothesis. *For. Ecol. Manag.* 355, 124-140 (2015).
- 286 16 Pugh, T. A. M. *et al.* Carbon emission from land-use change is substantially enhanced by
287 agricultural management. *Env. Res. Lett.*, 124008 (2015).

- 288 17 Guo, L. B. & Gifford, R. M. Soil carbon stocks and land use change: a meta analysis. *Glob.*
289 *Change Biol.* 8, 345-360 (2002).
- 290 18 Powlson, D. S. *et al.* Limited potential of no-till agriculture for climate change mitigation.
291 *Nat. Clim. Change* 4, 678-683 (2014).
- 292 19 Shevliakova, E. *et al.* Carbon cycling under 300 years of land use change: Importance of the
293 secondary vegetation sink. *Glob. Biogeochem. Cycles* 23, GB2022 (2009).
- 294 20 Stocker, B. D., Feissli, F., Strassmann, K. M., Spahni, R. & Joos, F. Past and future carbon
295 fluxes from land use change, shifting cultivation and wood harvest. *Tellus B* 66, 23188 (2014).
- 296 21 Wilkenskjeld, S., Kloster, S., Pongratz, J., Raddatz, T. & Reick, C. H. Comparing the
297 influence of net and gross anthropogenic land-use and land-cover changes on the carbon cycle
298 in the MPI-ESM. *Biogeosciences* 11, 4817-4828 (2014).
- 299 22 Friend, A. D. *et al.* Carbon residence time dominates uncertainty in terrestrial vegetation
300 responses to future climate and atmospheric CO₂. *Proc. Nat. Acad. Sci.* 111, 3280-3285
301 (2014).
- 302 23 Hansis, E., Davis, S. J. & Pongratz, J. Relevance of methodological choices for accounting of
303 land use change carbon fluxes. *Glob. Biogeochem. Cycles* 29, 1230-1246 (2015).
- 304 24 Pan, Y. *et al.* A Large and Persistent Carbon Sink in the World's Forests. *Science* 333, 988-
305 993 (2011).
- 306 25 Ahlström, A. *et al.* The dominant role of semi-arid ecosystems in the trend and variability of
307 the land CO₂ sink. *Science* 348, 895-899 (2015).
- 308 26 Erb, K.-H. *et al.* Bias in attributing of forest carbon sinks. *Nat. Clim. Change* 3, 854-856
309 (2013).

- 310 27 Schimel, D., Stephens, B. B. & Fisher, J. B. Effect of increasing CO₂ on the terrestrial carbon
311 cycle. *Proc. Nat. Acad. Sci.* 112, 436-441 (2015).
- 312 28 Ehlers, I. *et al.* Detecting long-term metabolic shifts using isotopomers: CO₂-driven
313 suppression of photorespiration in C-3 plants over the 20th century. *Proc. Nat. Acad. Sci.* 112,
314 15585-15590 (2015).
- 315 29 Sun, Y. *et al.* Impact of mesophyll diffusion on estimated global land CO₂ fertilization.
316 *Proceedings of the National Academy of Sciences*, doi:10.1073/pnas.1418075111 (2014).
- 317 30 Welp, L. R. *et al.* Interannual variability in the oxygen isotopes of atmospheric CO₂ driven by
318 El Nino. *Nature* 477, 579-582 (2011).
- 319 31 Ciais, P. *et al.* Large inert carbon pool in the terrestrial biosphere during the Last Glacial
320 Maximum. *Nat. Geosc.* 5, 74-79 (2012).
- 321 32 Beer, C. *et al.* Terrestrial Gross Carbon Dioxide Uptake: Global Distribution and Covariation
322 with Climate. *Science* 329, 834-838 (2010).
- 323 33 McMahon, S. M., Geoffrey G Parker, and Dawn R Miller. 2010. . Evidence for a recent
324 increase in forest growth. *Proc. Nat. Acad. Sci* 107, 3611–3615 (2010).
- 325 34 van der Sleen, P. *et al.* No growth stimulation of tropical trees by 150 Years of CO₂
326 fertilization but water-use efficiency increased. *Nat. Geosc.* 8, 24–28 (2015).
- 327 35 Pugh, T. A. M., Muller, C., Arneth, A., Haverd, V. & Smith, B. Key knowledge and data gaps
328 in modelling the influence of CO₂ concentration on the terrestrial carbon sink. *J. Plant Phys.*
329 203, 3-15 (2016).
- 330 36 Raymond, P. A. *et al.* Global carbon dioxide emissions from inland waters. *Nature* 503, 355-
331 359 (2013).

- 332 37 Regnier, P. *et al.* Anthropogenic perturbation of the carbon fluxes from land to ocean. *Nat.*
333 *Geosc.* 6, 597-607, doi:10.1038/ngeo1830 (2013).
- 334 38 Prestele, R. *et al.* Hotspots of uncertainty in land use and land cover change projections: a
335 global scale model comparison. *Glob. Change Biol.*, gcb.13337 (2016).
- 336 39 Bais, A. L. S., Lauk, C., Kastner, T. & Erb, K. Global patterns and trends of wood harvest and
337 use between 1990 and 2010. *Ecol. Econ.* 119, 326-337 (2015).
- 338 40 McGrath, M. J. *et al.* Reconstructing European forest management from 1600 to 2010.
339 *Biogeosciences* 12, 4291-4316 (2015).
- 340 41 Richter, D. D. & Houghton, R. A. Gross CO₂ fluxes from land-use change: implications for
341 reducing global emissions and increasing sinks. *Carb. Manag.* 2, 41-47 (2011).
- 342 42 Bayer, A. D., Lindeskog, M., Pugh, T. A. M., Fuchs, R. & Arneth, A. Uncertainties in the land
343 use flux resulting from land use change reconstructions and gross land transitions. *Earth Syst.*
344 *Dyn. Discuss.* (2016).
- 345 43 Korner, C. Slow in, rapid out - Carbon flux studies and Kyoto targets. *Science* 300, 1242-1243
346 (2003).
- 347 44 Krause, A., Pugh, T. A. M., Bayer, A. D., Lindeskog, M. & Arneth, A. Impacts of land-use
348 history on the recovery of ecosystems after agricultural abandonment. *Earth Syst. Dyn.* 7, 745-
349 766 (2016).
- 350 45 Zaehle, S., Jones, C. D., Houlton, B., Lamarque, J.-F. & Robertson, E. Nitrogen Availability
351 Reduces CMIP5 Projections of Twenty-First-Century Land Carbon Uptake. *J. Clim.* 28, 2494-
352 2511 (2015).
- 353 46 Seidl, R., Schelhaas, M. J., Rammer, W. & Verkerk, P. J. Increasing forest disturbances in
354 Europe and their impact on carbon storage. *Nat. Clim. Change* 4, 806-810 (2014).

- 355 47 Hantson, S. *et al.* The status and challenge of global fire modelling. *Biogeosciences* 13, 3359-
356 3375 (2016).
- 357 48 Running, S. W. Ecosystem disturbance, carbon, and climate. *Science* 321, 652-653 (2008).
- 358 49 Galik, C. S., Murray, B. C., Mitchell, S. & Cottle, P. Alternative approaches for addressing
359 non-permanence in carbon projects: an application to afforestation and reforestation under the
360 Clean Development Mechanism. *Mitigation and Adaptation Strategies for Global Change* 21,
361 101-118 (2016).
- 362 50 Friess, D. A., Phelps, J., Garmendia, E. & Gomez-Baggethun, E. Payments for Ecosystem
363 Services (PES) in the face of external biophysical stressors. *Glob. Env. Change* 30, 31-42
364 (2015).

365

366 **Corresponding Author**

367 Correspondence and request for materials should be addressed to Almut Arneth,
368 Almut.arneth@kit.edu

369

370 **Acknowledgements**

371 AA, ADB and TAMP acknowledge support from EU FP7 grants LUC4C (grant no. 603542) and
372 OPERAS (grant no.308393), and the Helmholtz Association in its ATMO programme and its impulse
373 and networking fund. MF, WL, CY and SS were also funded by LUC4C. JP and JEMSN were
374 supported by the German Research Foundation's Emmy Noether Program (PO 1751/1-1). EK was
375 supported by the ERTDF (S-10) from the Ministry of the Environment, Japan. ER was funded by
376 LUC4C and by the Joint UK DECC/Defra Met Office Hadley Centre Climate Programme (GA01101).
377 SZ has received funding from the European Research Council (ERC) under the European Union's
378 Horizon 2020 research and innovation programme (grant agreement no. 647204; QUINCY). BDS is
16

379 supported by the Swiss National Science Foundation and FP7 funding through project EMBRACE
380 (282672). PC received support from the ERC SyG project IMBALANCE-P ‘Effects of phosphorus
381 limitations on Life, Earth system and Society’ Grant agreement no.: 610028.’

382

383 **Author contributions**

384 AA, SS, JP, BS conceived the study. BP, LC, AB, MF, EK, JEMN, ADB, ML, TAMP, ER, TG, NV,
385 CY, SZ made changes to model code and provided simulation results. AA and SS analysed results.
386 BS, PC, WL provided Fig. 3. AA wrote the first draft, all authors commented on the draft and
387 discussion of results.

388 **Additional information**

389 Supplementary information is available in the online version of the paper. Reprints and permissions
390 information is available online at www.nature.com/reprints. Correspondence and requests for
391 materials should be addressed to A.A.

392

393 **Box 1: Calculations of global terrestrial carbon uptake and removal**

394 The net atmosphere-to-land carbon flux (F_L) is generally inferred as the difference between other
395 terms of the global carbon cycle perturbation:

$$396 \quad F_L = F_{FFC} - F_O - \frac{dA_{CO_2}}{dt} \quad (1)$$

397 where F_{FFC} are fossil fuel and cement emissions, F_O is the atmosphere-ocean carbon exchange
398 (currently an uptake) and $\frac{dA_{CO_2}}{dt}$ is the atmospheric growth rate of CO_2 (equation 1). F_{FFC} and $\frac{dA_{CO_2}}{dt}$ are
399 well known, and the estimate of the decadal global ocean carbon sink is bounded by a range of
400 observations¹ such that the net land carbon flux is relatively well constrained. By contrast, there is

401 much less confidence in separating F_L into a carbon flux from anthropogenic land use and land cover
402 change (F_{LULCC}), and a residual carbon flux to the land (F_{RL} , (equation 2)) which is typically calculated
403 as the difference from the other carbon-cycle components:

$$404 \quad F_L = F_{RL} - F_{LULCC} \quad (2)$$

405 F_{LULCC} and F_{RL} are both made up of source and sink fluxes. Uncertainties in F_{LULCC} and F_{RL} are around
406 35% - 40% over the period 1870-2014 (when expressed as % of the cumulative mean absolute values),
407 compared to 13% for the cumulative ocean sink and 5% for fossil fuel burning and cement emissions¹.

408 F_{LULCC} has been modelled by the bookkeeping method (combining data-driven representative carbon
409 stocks trajectories and/or, for the satellite period, remote-sensing information on carbon density for
410 different biomes, with estimates of land-cover change), or by dynamic global vegetation models
411 (DGVMs; calculating carbon density of ecosystems with process-based algorithms; see Methods).
412 DGVMs can also be used to calculate explicitly the magnitude and spatial distribution of F_{RL} (refs 1,
413 3) instead of deducing its global value as a difference between F_L and F_{LULCC} as done in global budget
414 analyses. The bookkeeping approach has the advantage that carbon densities and carbon response
415 functions that describe the temporal evolution and fate of carbon after a LULCC disturbance can be
416 based directly on observational evidence^{6,23}, but has to assume that local observations can be
417 extrapolated to regions/countries or biomes, thus partly ignoring spatial edaphic and climatic gradients
418 of carbon stocks. The DGVM-based simulations have the advantage to account for environmental
419 effects on carbon stocks through time, and account for spatial heterogeneity, but are poorly
420 constrained by data. DGVMs and bookkeeping models have similarly large degree of uncertainties¹.

421 **Figure captions**

422 Figure 1: Difference in LULCC emission flux (ΔF_{LULCC}) due to individual processes. **a**, Wood harvest.
423 **b**, Shifting cultivation. **c**, Harvest (using the grass functional type). **d**, Full crop representation.
424 Coloured lines represent different models, grey symbols and hairlines are average \pm one standard
425 deviation.

426 Figure 2: Response ratio of cumulative $F_{LULCC,1}$ and $F_{LULCC,0}$. See also Supplementary Table 1 and
427 methods for individual processes and models.

428 Figure 3: Comparison of net (a) and gross (b) forest / natural land change (million km²) between
429 different LULCC data sets. Changes in LUH1 data ⁷ represents the change of natural land because
430 there is no separate forest type in LUH1 while change in the other data sets indicates the forest change.

431 **Methods**

432 **General simulation setup**

433 Carbon fluxes from land-use change are derived as the difference between a simulation with
434 historically varying observed climate, atmospheric CO₂ concentration and land-cover change (S3) and
435 one in which land-cover change was held constant (S2)^{1,2}. Land-cover changes were taken from
436 HYDE⁵¹ or LUH1⁷. In S2, land-cover distribution was fixed. Gridded historical estimates of gross-
437 transitions (shifting cultivation (SC) in the tropics) and wood harvesting (WH) were taken from ref. 7.

438 Spin-up used repeated climate from the first decades of the twentieth century, and constant CO₂
439 concentration and land-cover distribution (for details, see the individual description below). Upon
440 achieving steady-state, land-cover distribution and CO₂ concentration were allowed to evolve
441 transiently, whereas transient climate evolution began at 1901. Atmospheric CO₂ concentration was
442 taken from ice core data until roughly mid-twentieth century, when atmospheric measurements
443 became available¹. A “baseline” carbon flux related to land-use change ($F_{LULCC,0}$; see Supplementary
444 Table 1) is defined as excluding gross transitions and wood harvest, and using the grass plant
445 functional type to represent crop areas. Data in this Perspective were from previously published work,
446 supplemented by additional, new simulations. In cases where more than one of the processes that are
447 under investigation here were assessed by one model, several S3 experiments were provided.
448 Although spin-up and model configurations differed between models, for S2 and S3 simulations of
449 any one individual model the setup was the same, which allows to identify the effect of adding the
450 individual processes. We describe briefly the relevant aspects of models and simulational protocol, in
451 particular where they differ from their previously published versions.

452 **JULES model.** Here, to implement crop harvest, four additional PFTs were added: C3 crops, C4
453 crops, C3 pasture and C4 pasture, with identical parameter sets as the C3 and C4 grass PFTs. Lotka-
454 Volterra equations⁵² are used three times to calculate the vegetation distribution in natural areas, crop
455 and pasture areas, with the calculations in each area being independent of the others. Crop-harvest is

456 represented by diverting 30% of crop litter to the fast product pool instead of to the soil; the fast
457 product pool has a rapid decay timescale of 1 year. Pasture is not harvested.

458 The model is forced by crop and pasture area from the Hyde 3.2 dataset¹ and by CRU-NCEP
459 climate^{1,2}, both at 1.875x1.25 degrees, using an hourly time-step, and updating vegetation distribution
460 every ten days. 1080 years of spin-up were run by fixing crop and pasture areas at 1860 levels and by
461 repeating 1901-1920 climate and CO₂ concentrations.

462 **JSBACH model.** The JSBACH version used here is similar to the version in ref.1. S3 experiments
463 include gross land-use transitions and WH²¹. $F_{LULCCc,0}$ in Supplementary Table 2 were calculated by
464 subtracting the individual contributions of these processes. Net transitions are derived from the gross
465 transition implementation, but by minimizing land conversions²¹. WH⁷ is taken not only from forest
466 PFTs but also shrubs and natural grasslands are harvested. Upon harvest, 20% of the carbon is
467 immediately released to the atmosphere; the rest is transferred into the litter and subject to soil
468 dynamics. JSBACH simulations were conducted at 1.9°x1.9° forced with remapped 1° LUH1 data
469 from 1860-2014 and daily climate calculated from the 6-hourly 0.5° CRU-NCEP product¹ for the
470 years 1901-2014. The initial state in 1860 is based on a spin-up with 1860 CO₂ concentrations (286.42
471 ppm), cycling (detrended) 1901-1921 climate and constant 1860 LUH1 WH amounts. From 1860
472 annual CO₂ forcing was used, and after 1901 climate was taken from CRU-NCEP. In the no-harvest
473 simulation the 1860 WH amounts were applied throughout the whole simulated period.

474 **LPJ-GUESS model.** SC: For implementing SC, recommendations followed those by ref.7, with
475 rotation periods of 15 years. Simulations used the coupled carbon-nitrogen version of the model^{16,53}
476 spin-up used constant 1701 land-cover and CO₂ concentration, and 1901-1930 recycled climate. Upon
477 steady-state land-cover and CO₂ were allowed to change from 1701, and climate from 1901 onwards⁴².
478 When land is cleared, 76% of woody biomass and 71% of leaf biomass is removed and oxidised
479 within one year, with a further 21% of woody biomass assigned to a product pool with 25 year
480 turnover time⁴². Upon abandonment a secondary forest stand is created and recolonization of natural

481 vegetation takes place from a state of bare soil. With forest rotation, young stands (above a minimum
482 age of 15 years) are preferentially converted.

483 GH/MC: Simulations are taken from ref. 16, using the carbon-only version of the model. 68% of
484 deforested woody biomass and 75% of leaf biomass is oxidised within one year, with a further 30% of
485 woody biomass going to the product pool. In the GH case, 50% of the above-ground biomass are
486 annually removed from the ecosystem. In MC, 90% of the harvestable organs and an additional 75%
487 of above-ground crop residues are removed each year. Simulations ran from 1850 to 2012, with 1850
488 land-cover and CO₂ concentrations, and recycled climate (1901-1930) being used for spin-up. All LPJ-
489 GUESS simulations used CRU TS 3.23 climate⁵⁴.

490 **LPJ model.** Compared to previous versions, the model now uses the World Harmonization Soils
491 Database v.1.2 for soil texture and Cosby equations⁵⁵ to estimate soil water holding capacity. Further
492 developments allow for gross land-use transitions and WH to be prescribed. Changes include: (1) the
493 primary grid-cell fraction only decreases in size; (2) secondary grid-cell fractions can decrease or
494 increase in size by combining with other secondary forest fractions, recently abandoned land, or
495 fractions with recent WH; (3) deforestation that results in an immediate flux to the atmosphere equal
496 to 100% of heartwood biomass and 50% of sapwood biomass; root biomass enters belowground litter
497 pools, while 100% leaf and 50% of sapwood biomass becomes part of aboveground litter.

498 WH demand⁷ on primary or secondary lands was met by the biomass in tree sapwood and heartwood
499 only. Only whole trees were harvested (that is, tree-density was reduced); wood from deforestation
500 was not included to meet WH demand. 100% of leaf biomass and 40% of the sapwood and heartwood
501 enters the aboveground litter, and 100% of root biomass enters the belowground litter pools; 60% of
502 sapwood and heartwood are assumed to go into a product pool. Of these, 55% go to the 1-year product
503 pool (emitted in the same year), 35% go to the 10-year product pool (emitted at rate 10% per year) and
504 10% go to the 100-year product pool (emitted at rate 1% per year). These delayed pool-emission
505 fluxes are part of the LULCC fluxes. After harvest, the harvested fraction is mixed with existing
506 secondary forest fraction, or a secondary fraction is created if none exists, while fully conserving

507 biomass. For simulations with SC, grid-cell fractions that underwent land-use change were not mixed
508 with existing managed lands or secondary fractions until all land-use transitions had occurred.

509 Simulations were performed using monthly CRU⁵⁴ (TS v.3.23) climate at 0.5° degrees, and finished in
510 year 2013. Spin-up was done using recycled 1901-20 climate, and using 1860 land-cover and CO₂.
511 Upon steady-state, land cover and CO₂ varied after 1860 and climate varied after 1900.

512 **LPJmL model.** The LPJmL version used was as described in refs 56-58. In the baseline scenario all
513 crops were simulated as a mixture of C3 and C4 managed grasslands, 50% of the aboveground
514 biomass is transferred to the harvest compartment and assumed to be respired in the same year.
515 Climate data was 1901-2014 CRU TS v.3.23 monthly datasets and land-use patterns from the HYDE
516 3.2 dataset. Simulations were performed at 0.5° spatial resolution. Model spin-up used recycled
517 climate data from 1901-1920, and with land use patterns and CO₂ concentrations fixed to the 1860
518 value. Simulations from 1861-2014 were done with varying annual CO₂ concentration values, and
519 varying land use patterns according to the HYDE dataset, and with transient climate from 1901 until
520 2014.

521 **LP3X model.** Land-use change, including SC and WH, is implemented as described in ref. 20,
522 using the full land-use transition and wood harvesting data provided⁷. Wood (heartwood and
523 sapwood) removed by harvesting and land conversion is diverted to products pools with
524 turnover rates of 2 years (37.5%) and 20 years (37.5%). The rest, including slash from roots
525 and leaves is respired within the same year.

526 Simulation results shown here are based on employing the GCP 2015 protocol and input
527 data¹. LPX includes interactive C and N cycling with N deposition and N fertiliser inputs⁵⁹.
528 Simulations with SC and WH were spun up to equilibrium under land-use transitions and WH
529 of year 1500²⁰. Varying land-use transitions and WH was included from 1500 onwards, with
530 CO₂ and N deposition of year 1860 and recycled climate from CRU TS v.3.23, years 1901-
531 1931. All simulations are done on a 1 x 1 degree spatial resolution and make use of monthly

532 climate input. Original GCP standard input files were aggregated to 1 x 1 degrees conserving
533 area-weighted means (climate input) or absolute area of cropland and pasture (land use input).

534 **OCN model.** The OCN version used here is applied as in the framework of the annual carbon budget¹.
535 OCN includes interactive C and N cycling with N deposition and N fertiliser inputs⁶⁰. Wood harvest
536 was implemented by first satisfying the prescribed wood extraction rate from wood production due to
537 land-use change, and then removing additional biomass proportionally from forested tiles. Wood
538 (heartwood and sapwood) removed by harvesting and land conversion is diverted to products pools
539 with turnover rates of 1 years (59.7%), 10 years (40.2% for tropical, and 29.9% for extratropical trees)
540 and 100 years (10.4 % for extratropical trees)⁶¹. The remainder enters the litter pools. In case OCN's
541 forest growth rate did not suffice to meet the prescribed wood extraction rate, harvesting was limited
542 to 5% of the total stand biomass and assumed to stop if the stand biomass density fell below 1 kg C m⁻².
543 These limits were set to account for offsets in annual wood production between OCN's predicted
544 biomass growth and the assumptions in the Hurtt et al. database⁷. These limits may lead to lower than
545 prescribed WH rates in low productive areas. An additional run was performed with keeping WH
546 constant at 1860s level.

547 Simulations with WH were spun up to equilibrium using harvesting of the year 1860¹. Varying land-
548 use transitions or WH was included from 1860 onwards, with CO₂ and N deposition of year 1860 and
549 recycled climate from CRU-NCEP, years 1901-1931. All simulations are done on a 1 x 1 degree
550 spatial resolution and make use of daily climate input, which is disaggregated to half-hourly values by
551 means of a weather generator⁶². Original GCP standard input files were aggregated to 1 x 1 degrees
552 conserving area-weighted means (climate input) or absolute area of cropland and pasture (land use
553 input).

554

555 **ORCHIDEE model.** WH: Developments to the version included in ref.1 include annual WH, the total
556 wood harvested of a grid cell is removed from above-ground biomass of the different forest PFTs
557 proportional (i) to its fraction in the gridcell and (ii) also to its relative biomass among forest PFTs.

558 This results in harvesting more wood in biomass-rich forests. In cases of inconsistencies between the
559 Orchidee and Hurtt forest fraction, and to avoid forest being degraded from excessive harvest we
560 assume that no more than 20% of the total forest biomass of a gridcell can be harvested in one year.
561 Hence the biomass actually harvested each year can be slightly lower than prescribed⁷. The harvested
562 biomass enters three pools of 1, 10 and 100 residence years respectively (and is part of F_{LULCC}). Model
563 runs were done at $0.5^\circ \times 0.5^\circ$ resolution. Spin-up used recycled climate of 1901-1910. CO_2
564 concentration, land-cover and WH of the year 1860. The model was run until the change in mean total
565 carbon of 98% of grid-points over a ten-year spin-up period was $< 0.05\%$.

566 SC: Land cover transition matrices are upscaled from 0.5° LUH1 data⁷ so no transition information is
567 lost in the low-resolution run. The minimum bi-directional fluxes between two land cover types in
568 LUH1 were treated as shifting cultivation. The model was forced with CRU-NCEP forcing (v5.3.2),
569 re-gridded to 5° resolution from the original 0.5° resolution. Spin-up simulation used recycled climate
570 data for 1901-1910 with atmospheric CO_2 held at 1750 level, and land cover fixed at 1500. Transient
571 runs started from 1501 until 2014, with CO_2 varying from 1750 and climate varying from 1901. In the
572 transient run for the control simulation, land cover is held constant at 1500; for the SC run, land cover
573 varies by applying annual land use transition matrices of SC. All runs have been performed with
574 outputs on annual temporal resolution but forcing data is 6-hourly.

575 **OSCAR model.** A complete description of OSCAR v2.2 is provided by ref. 63. OSCAR is not a
576 DGVM, but a compact Earth system model calibrated on complex models. Here, it is used in an
577 offline setup in which the terrestrial carbon-cycle module is driven by exogenous changes in
578 atmospheric CO_2 (IPCC AR5 WG1 Annex 2), climate (CRU TS v.3.23), and land-use and land cover
579 (HYDE v.3.2).

580 The global terrestrial biosphere is disaggregated into nine regions (detailed by ref. 64) and subdivided
581 into five biomes (bare soil, forest, shrubland+grassland, cropland, pasture). The carbon-cycle in each
582 of these 45 subparts is represented by a three-box model whose parameters are calibrated on DGVMs.
583 The preindustrial equilibrium (carbon densities and fluxes) is calibrated on TRENDY models². The

584 transient response of NPP, heterotrophic respiration and wildfires to CO₂ and/or climate is calibrated
585 on CMIP5 models⁶⁵. The impact of land-use and land-cover change on the terrestrial carbon-cycle is
586 modelled using a bookkeeping approach. Coefficients used to allocate biomass after land-use or land-
587 cover change are based on ref. 66.

588 Since OSCAR v2.2 is meant to be used in a probabilistic setup we made an ensemble of 2400
589 simulations in which the parameters (for example, preindustrial equilibrium, transient responses,
590 allocation coefficients) are drawn randomly from the pool of available parameterizations. See ref. 63
591 for more details. The resulting OSCAR values discussed and shown in the main text are the median of
592 this ensemble.

593 **VISIT model.** Implementation of climate, land-use change (gross transitions, SC) and WH has not
594 changed from¹. Land-use, land-use change, and WH data for 1860-2014 were from LUH1⁷. For WH,
595 the amount of harvested biomass prescribed in ref. 7 were transferred from simulated stem biomass to
596 1-year product pool (emitted in entirety in same year of wood harvest), 10-year product pool, and 100-
597 year product pool in a same manner as in the cleared biomass with land-use change described in ref.
598 67. The non-harvested part of biomass remains in the ecosystem. The fluxes from WH pools are
599 included in the NBP calculations.

600 Climate data was 1901-2014 monthly CRU TS v.3.23 and all simulations were conducted with 0.5°
601 spatial resolution. The model spin-up was performed recycling climate data from 1901-1920, and with
602 land use patterns and CO₂ concentrations fixed to the 1860 value. Simulations from 1860-2014 were
603 done with varying annual CO₂ concentration values, varying land use patterns according to LUH1,
604 recycling the climate from 1901-1920 in the period 1860-1900, and with transient climate from 1901
605 until 2014.

606

607 **Data in Fig. 3.** Data for net forest change from the Food and Agriculture Organization (FAO)⁶⁸ is
608 calculated as the difference of forest area between 2000 and 2010 in each region. The same data were

609 also used in the Houghton et al. bookkeeping model⁶. The net forest change from Hansen et al.⁶⁹ is
610 based on satellite observations, and is their difference between gross forest gain and gross forest loss
611 during 2000-2012. Because the LUH1 dataset⁷ only has one type of natural vegetation, and does not
612 separate natural forest from natural grassland, the change in Fig. 3 represents the total change of
613 natural land. In Fig. 3b, for LUH1 the gross loss includes transitions from primary/secondary
614 vegetation to cropland / pasture, while the gross gain is the sum of transitions from cropland and
615 pasture to secondary land. With grasslands and forests treated as separate land-cover types in LUH2
616 (<http://luh.umd.edu/>), the change includes transitions from primary / secondary forest to cropland /
617 pasture (gross loss) and transitions from cropland / pasture to secondary forest (gross gain). The net
618 change for LUH1 or LUH2 is the difference between gross loss and gross gain. To be consistent with
619 ref. 69, the period calculated for LUH1 and LUH2 is also from 2000 to 2012. The products shown in
620 Figure 3 use definitions of forest loss and gain, and interpretation of differences between products
621 should therefore take these into consideration.

622

623 **Data and code availability.** The data that support the findings of this study are available upon
624 request, for access please contact almut.arneth@kit.edu and s.a.sitch@exeter.ac.uk. We are unable to
625 make the computer code of each of the models associated with this paper freely available because in
626 many cases the code is still under development. However, individual groups are open to share code
627 upon request, in case of interest please contact the co-authors for specific models. Access for LUH1 &
628 LUH2 is under <http://luh.umd.edu/data.shtml>; the HYDE data are accessible via
629 <http://themasites.pbl.nl/tridion/en/themasites/hyde/download/index-2.html>

630

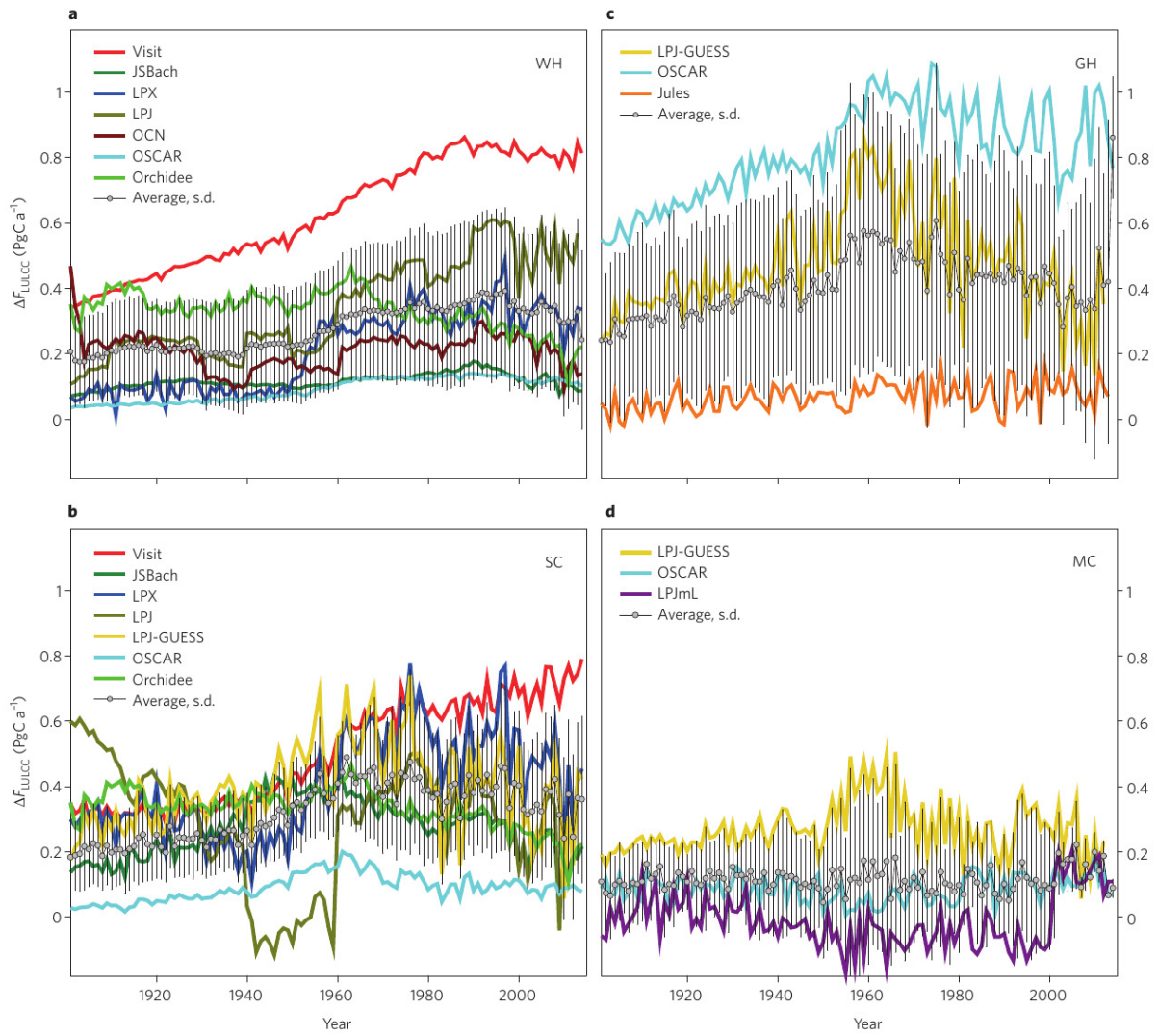
631 **References**

- 632 51 Klein Goldewijk, L., Beusen, A., van Drecht, G. & de Vos, M. The HYDE 3.1 spatially
633 explicit database of human-induced global land use change over the past 12,000 years. *Globl
634 Ecol. Biogeogr.* **20**, 73–86 (2011).
- 635 52 Clark, D. B. *et al.* The Joint UK Land Environment Simulator (JULES), model description –
636 Part 2: Carbon fluxes and vegetation dynamics. *Geosci. Model Dev.* **4**, 701-722 (2011).
- 637 53 Smith, B. *et al.* Implications of incorporating N cycling and N limitations on primary
638 production in an individual-based dynamic vegetation model. *Biogeosciences* **11**, 2027-2054
639 (2014).
- 640 54 Jones, P. & Harris, I. University of East Anglia Climatic Research Unit, CRU TS3. 21:
641 Climatic Research Unit (CRU) Time-Series (TS) Version 3.21 of High Resolution Gridded
642 Data of Month-by-month Variation in Climate (Jan. 1901—Dec. 2012). *NCAS British
643 Atmospheric Data Centre* (2013).
- 644 55 Cosby, B. J., Hornberger, G. M., Clapp, R. B. & Ginn, T. R. A STATISTICAL
645 EXPLORATION OF THE RELATIONSHIPS OF SOIL-MOISTURE CHARACTERISTICS
646 TO THE PHYSICAL-PROPERTIES OF SOILS. *Water Resources Res.* **20**, 682-690 (1984).
- 647 56 Bondeau, A. *et al.* Modelling the role of agriculture for the 20th century global terrestrial
648 carbon balance. *Glob. Change Biol.* **13**, 679-706 (2007).
- 649 57 Fader, M., von Bloh, W., Shi, S., Bondeau, A. & Cramer, W. Modelling Mediterranean agro-
650 ecosystems by including agricultural trees in the LPJmL model. *Geosc. Model Dev.* **8**, 3545-
651 3561 (2015).
- 652 58 Waha, K., van Bussel, L. G. J., Müller, C. & Bondeau, A. Climate-driven simulation of global
653 crop sowing dates. *Glob. Ecol. Biogeogr.* **12**, 247–259 (2012).

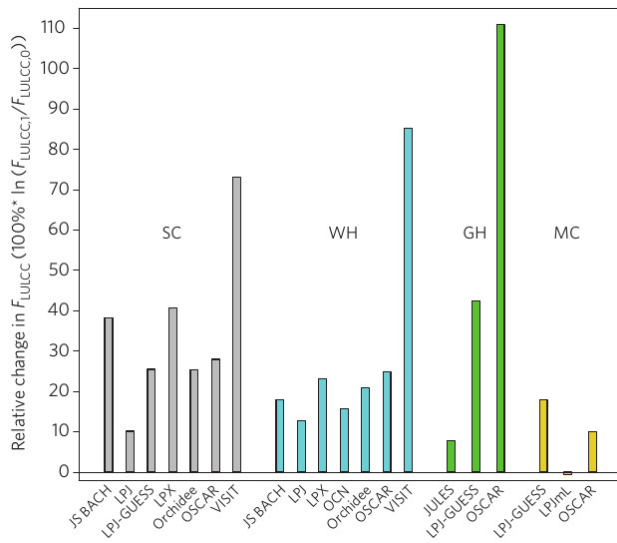
- 654 59 Stocker, B. D. *et al.* Multiple greenhouse-gas feedbacks from the land biosphere under future
655 climate change scenarios. *Nat. Clim. Change* **3**, 666-672 (2013).
- 656 60 Zaehle, S., Ciais, P., Friend, A. D. & Prieur, V. Carbon benefits of anthropogenic reactive
657 nitrogen offset by nitrous oxide emissions. *Nat. Geosc.* **4**, 601-605 (2011).
- 658 61 McGuire, A. D. *et al.* Carbon balance of the terrestrial biosphere in the twentieth century:
659 Analysis of CO₂, climate and land use effects with four process-based ecosystem models.
660 *Glob. Biogeochem. Cycles* **15**, 183-206 (2001).
- 661 62 Krinner, G., Ciais, P., Viovy, N. & Friedlingstein, P. A simple parameterization of nitrogen
662 limitation on primary productivity for global vegetation models. *Biogeosciences Discussions*
663 **2**, 1243-1282 (2005).
- 664 63 Gasser, T. *et al.* The compact Earth system model OSCAR v2.2: description and first results.
665 *Geosc. Model Dev.* **submitted** (2016).
- 666 64 Houghton, R. A. & Hackler, J. L. Carbon flux to the atmosphere from land-use changes: 1850
667 to 1990. (Carbon Dioxide Information Analysis Center, Oak Ridge, Tennessee, 2001).
- 668 65 Arora, V. K. *et al.* Carbon-Concentration and Carbon-Climate Feedbacks in CMIP5 Earth
669 System Models. *J. Clim.* **26**, 5289-5314 (2013).
- 670 66 Mason, E. J., Yeh, S. & Skog, K. E. Timing of carbon emissions from global forest clearance.
671 *Nature Clim. Change* **2**, 682-685 (2012).
- 672 67 Kato, E., Kinoshita, T., Ito, A., Kawamiya, M. & Yamagata, Y. Evaluation of spatially
673 explicit emission scenario of land-use change and biomass burning using a process-based
674 biogeochemical model. *J. Land Use Sc.* **8**, 104-122 (2013).
- 675 68 *Global Forest Resources Assessment 2010*. (FAO, 2010).

676 69 Hansen, M. C. *et al.* High-Resolution Global Maps of 21st-Century Forest Cover Change.
677 *Science* **342**, 850-853 (2013).

678

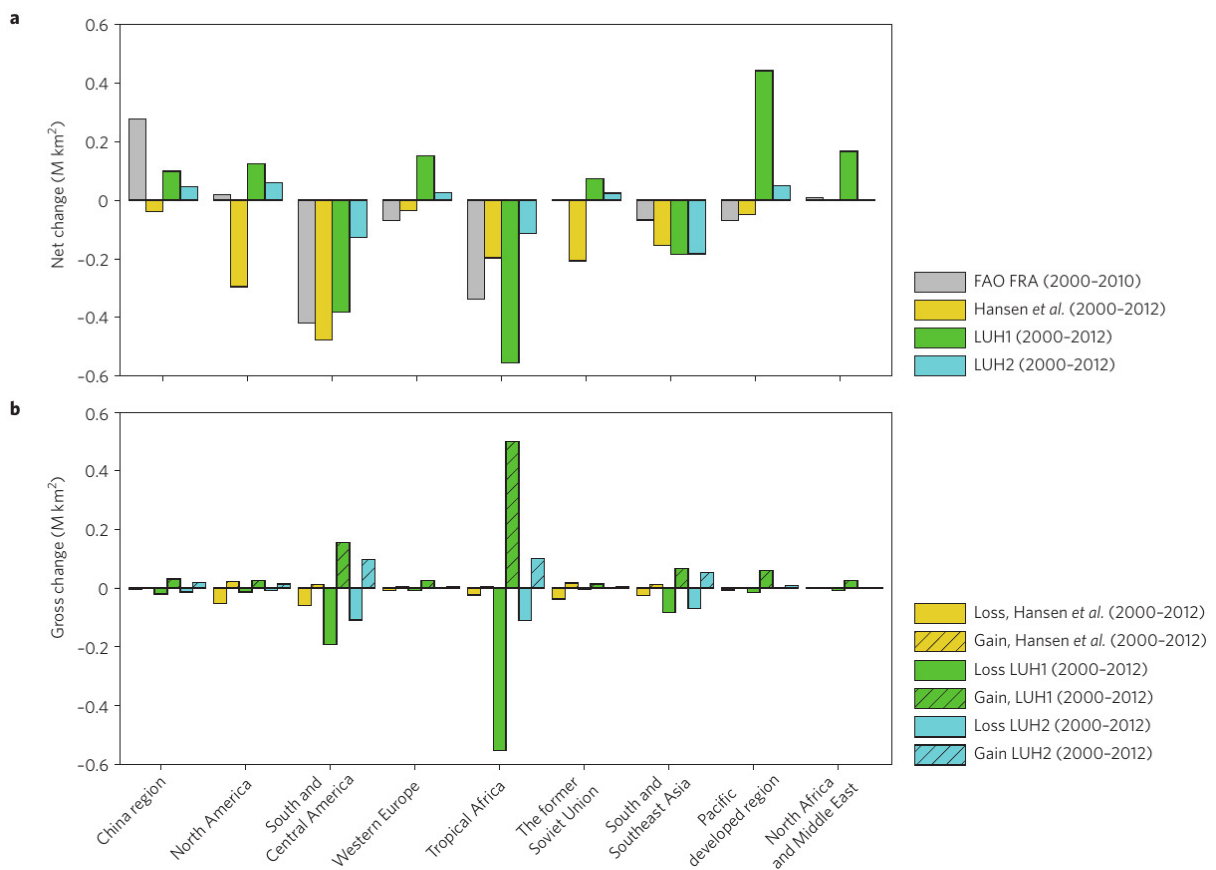


682 Figure 2



683

684 Figure 3



685